

# **Image Current Heating on Metal Surface Due to Charged Bunches**

Xintian E. Lin and David H. Whittum

Submitted to Physical Review Special Topics - Accelerators and Beams

---

*Stanford Linear Accelerator Center, Stanford University, Stanford, CA 94309*

Work supported by Department of Energy contract DE-AC03-76SF00515.

# Image Current Heating on Metal Surface Due to Charged Bunches

Xintian E. Lin and David H. Whittum

*Stanford Linear Accelerator Center, Stanford University, Stanford, CA 94309*

(Dated: February 18, 2000)

When charged particles pass through a metal pipe, they are accompanied by an image current on the metal surface. With intense short bunches passing near the metal surface, the peak image current density can be very high. This current may result in substantial temperature rise on the surface, especially in multi-bunch operation. In this paper, we derive an explicit formula for the surface temperature rise due to this previously unrecognized effect, and show that it should be taken into account in structure and collimator design for future accelerators.

PACS numbers: 41.20.-q, 44.10.+i

## I. INTRODUCTION

In high energy accelerators, beams are brought to the collision point and collision products are detected. To reduce background noise, well defined beams are highly desirable. However, due to intra beam and inter beam interaction, the beams at the end of the long accelerator usually have distorted shapes and beam halo may form as well. Therefore, a collimation section is placed before interaction point, as illustrated in Fig. 1. Damage to the

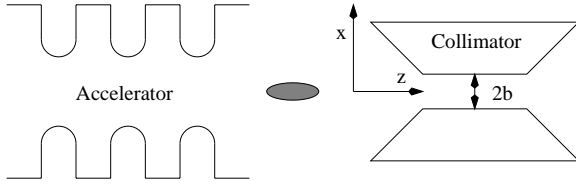


FIG. 1: Post linac Collimation.

collimator surface, which is observed in SLC operation[1], is a prime consideration in engineering design. For effective collimation, the aperture,  $2b$ , is usually chosen to be about  $10\sigma_x$ . The choice of beam transverse size  $\sigma_x$  at collimation, and consequently  $2b$ , is then restricted by several factors, including wakefield generated by small aperture, the possible damage to the collimator due to the energy density of the beams and magnet designs to achieve the proper beta function. In this article we will introduce another effect that limits the peak current and beam size. It is a result of the pulsed surface heating induced on the collimator surface by the image current.

## II. SINGLE BUNCH PULSED HEATING

Taking a cylindrical pipe for example (Fig. 2), the maximum surface magnetic field due to a relativistic charged

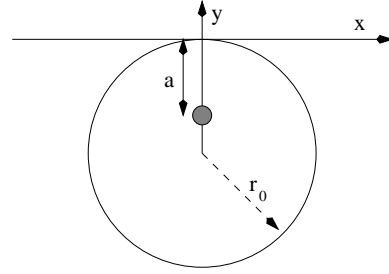


FIG. 2: Electron bunch passing through a smooth pipe.

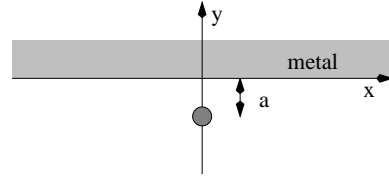


FIG. 3: Electron bunch passing close to a surface pipe.

bunch moving in  $z$  direction is

$$H_x(x=0, y=0) = -\frac{I}{2\pi} \left( \frac{1}{a} + \frac{1}{r_0} \frac{r_0 - a}{a} \right), \quad (1)$$

where  $a$  is the distance from the pipe wall, and the bunch current  $I$  can be written in the form

$$I(z, t) = \frac{Qc}{\sqrt{2\pi}\sigma_z} e^{-(z-ct)^2/2\sigma_z^2}, \quad (2)$$

where  $Q$  represents bunch charge. A Gaussian bunch with length  $\sigma_z$  is assumed. In the limit of  $a \ll r_0$ , the field is well approximated by that of an infinite flat surface (Fig. 3),

$$H_x(x, y=0) = -\frac{I}{\pi} \frac{a}{a^2 + x^2}. \quad (3)$$

Inside metals, Maxwell's equations reduce to a diffu-

sion equation

$$\nabla^2 H_x = -\sigma \mu_0 \frac{\partial H_x}{\partial t}, \quad (4)$$

where the displacement current term  $\partial D/\partial t$  is negligible. The electric conductivity is represented by  $\sigma$ . In the frequency domain, we have

$$\left(\frac{\partial^2}{\partial x^2} + \frac{\partial^2}{\partial y^2} + \frac{\partial^2}{\partial z^2}\right) \tilde{H}_x = j\omega \sigma \mu \tilde{H}_x \quad (5)$$

with boundary condition from Eq. (3)

$$\tilde{H}_x(x, y=0, z, \omega) = -\frac{\tilde{I}(z, \omega)}{\pi} \frac{a}{a^2 + x^2}, \quad (6)$$

where the Fourier transform of current

$$\tilde{I}(z, \omega) = \int_{-\infty}^{+\infty} I(z, t) e^{-j\omega t} dt = Q e^{-\omega^2/2\omega_\sigma^2} e^{-j\omega z/c}. \quad (7)$$

The characteristic frequency spread  $\omega_\sigma = c/\sigma_z$ . An order of magnitude estimation gives  $\partial^2/\partial x^2 \approx 1/a^2$  and  $\partial^2/\partial z^2 \approx 1/\sigma_z^2$ . With  $a \approx 1 \text{ mm}$ ,  $\sigma_z \approx 125 \text{ }\mu\text{m}$  and  $\omega_\sigma \sigma \mu \approx 1/(80 \text{ nm})^2 \gg (1/a^2, 1/\sigma_z^2)$  [9]. Eq. (5) simplifies to

$$\frac{\partial^2}{\partial y^2} \tilde{H}_x = j\omega \sigma \mu \tilde{H}_x. \quad (8)$$

Together with Eq. (6), we obtain the solution

$$\tilde{H}_x(x, y > 0, z, \omega) = -\frac{\tilde{I}(z, \omega)}{\pi} \frac{a}{a^2 + x^2} e^{-\frac{1+j}{\delta} y} \quad (9)$$

with skin depth  $\delta = \sqrt{2/\omega \mu \sigma}$ .

The current density  $\tilde{J}_z$  inside the metal is related to the magnetic field by

$$\tilde{J}_z = \frac{\partial \tilde{H}_x}{\partial y} = \tilde{H}_x \left(-\frac{1+j}{\delta}\right). \quad (10)$$

The resulting ohmic heating,  $|\tilde{J}_z|^2/\sigma$ , gives rise to a power spectrum density

$$\tilde{P}_d(x, y, z, \omega) = \left(\frac{|\tilde{I}(z, \omega)|}{\pi}\right)^2 \left(\frac{a}{a^2 + x^2}\right)^2 \frac{1}{\sigma} \frac{2}{\delta^2} e^{-2y/\delta}, \quad (11)$$

which is integrated over frequency to obtain the total energy density deposited by a single bunch

$$\begin{aligned} E_d(x, y, z) &= \int_{-\infty}^{+\infty} \tilde{P}_d(x, y, z, \omega) \frac{d\omega}{2\pi} \\ &= \frac{Z_0 c}{2\pi} \left(\frac{Q}{\sigma_z}\right)^2 \frac{1}{\pi^2} \left(\frac{a}{a^2 + x^2}\right)^2 g(y/\delta(\omega_\sigma)). \end{aligned} \quad (12)$$

The penetration function

$$\begin{aligned} g(u) &= \int_0^\infty e^{-z} e^{-2uz^{1/4}} dz \\ &= \frac{2}{(2\pi)^{3/2}} G_{4\ 1}^1 \left[ \frac{u^4}{16} \left| \begin{matrix} [0] \\ [0, 1/4, 1/2, 3/4] \end{matrix} \right. \right] \end{aligned} \quad (13)$$

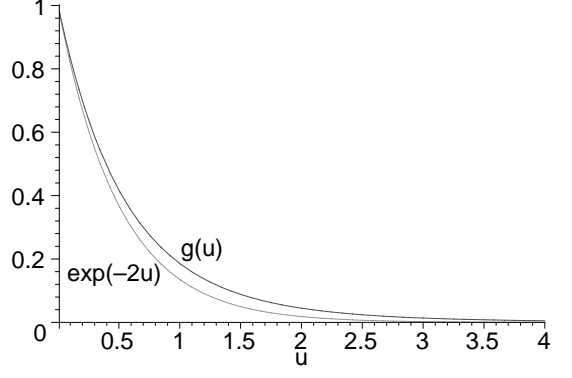


FIG. 4: Penetration function  $g(u)$ , and  $e^{-2u}$ .

is expressed in Meijer's G function[2]. The values of  $g(u)$  and  $e^{-2u}$  are plotted in Fig. 4. There are a few points worth noting. First,  $g(0) = 1$ . Second, at large  $u$ ,  $g(u) \rightarrow 3/2u^4$ . The penetration function has a longer tail than the exponential. Comparing the integral  $\int_0^\infty g(u) du = \Gamma(3/4)/2 \approx 0.6127$  and  $\int_0^\infty e^{-2u} du = 0.5$ , it is clear that  $e^{-2u}$  underestimates the total energy by about 18%. For a better approximation of  $g(u)$ , we may use  $e^{-2u/\Gamma(3/4)}$ , i.e. replacing the argument  $y/\delta(\omega_\sigma)$  by  $y/\delta_e$ , where the effective skin depth  $\delta_e = \Gamma(3/4)\delta(\omega_\sigma)$  accounts for the greater penetration. The exact and approximate solutions are compared in Fig. 5. We will use the effective skin depth in later sections.

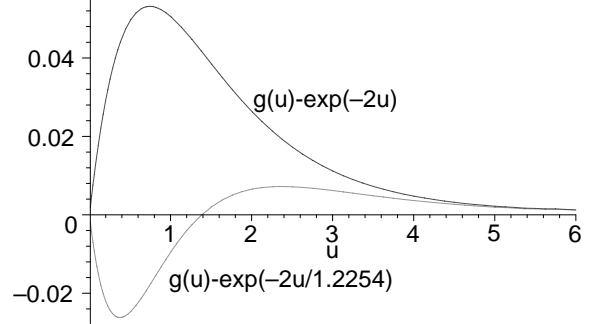


FIG. 5: Difference between  $g(u)$  and  $e^{-2u}$ ,  $e^{-2u/1.2254}$

In writing Eq. (12), we have ignored the heat diffusion over the time scale  $\Delta t \approx \sigma_z/c$ . This is a good approximation as long as thermal diffusion length is much smaller than the RF skin depth, i.e.

$$l_{diff} = \sqrt{\frac{K}{C_p} \Delta t} = \sqrt{\frac{K}{C_p} \frac{\sigma_z}{c}} \ll \delta(\omega_\sigma) = \sqrt{\frac{2}{\mu \sigma} \frac{\sigma_z}{c}}, \quad (14)$$

which reduces to

$$\sqrt{\frac{K\mu\sigma}{2C_p}} \ll 1, \quad (15)$$

where  $K$  and  $C_p$  are the thermal conductivity and volume specific heat respectively. Taking copper and titanium for example,  $\sqrt{K\mu\sigma/2C_p} = 0.065$  and  $3.8 \times 10^{-3}$  respectively. It shows that Eq. (14) is an excellent assumption for most metals since copper has one of the highest  $K$  and  $\sigma$  of all metals.

To a very good approximation, the single electron bunch pulsed heating can be considered as an instantaneous energy deposition. The instantaneous temperature rise is then

$$\begin{aligned} T_1(x, y, z) &= \frac{E_d(x, y, z)}{C_p} \\ &= \frac{Z_0 c}{2\pi} \left(\frac{Q}{\sigma_z}\right)^2 \frac{1}{\pi^2} \left(\frac{a}{a^2 + x^2}\right)^2 \frac{g(y/\delta(\omega\sigma))}{C_p}. \end{aligned} \quad (16)$$

It is notable that the peak temperature is independent of the electrical conductivity. The resistive loss and penetration depth are both inversely proportional to the square root of conductivity, and therefore the ratio, energy density, is constant. In our future collider design[3], a titanium spoiler with  $r_0 = 2mm$  is located in the post-linac collimation section. Taking  $Q = 1.52nC$ ,  $\sigma_z = 125\mu m$ ,  $C_p = 2.36J/cm^3$ [4] and assuming  $a = r_0$ , Eq. (16) gives  $T_1(0) = 0.029^\circ C$ . In fact, when the beam is at the center of the circular pipe, Eq. (3) overestimates surface magnetic field by a factor of 2 compared with Eq. (1). The temperature rise should be  $T_1(0) = 0.007^\circ C$ .

### III. MAXIMUM SINGLE BUNCH PULSE HEATING

The above example shows that under normal conditions, such a spoiler is quite safe. However, the spoiler is also part of the machine protection system, and is required to survive in the worst case, a full bunch train impact. Such an event corresponds to beam missteering/dumping or equipment failure[3]. Under those circumstance the electron bunches can get very close to, even into the metal surface.

Let's consider a bunch with Gaussian transverse distribution (Fig. 6)

$$\tilde{I}(x, y, z, \omega) = \tilde{I}(z, \omega) \frac{e^{-x^2/2\sigma_x^2}}{\sqrt{2\pi}\sigma_x} \frac{e^{-(y+a)^2/2\sigma_y^2}}{\sqrt{2\pi}\sigma_y}. \quad (17)$$

Since the electron bunch current in the region  $y > 0$  is neutralized by a corresponding image current inside the metal, they do not contribute to the magnetic field at  $y = 0$ . And due to its low current density compared to the surface image current density ( $1/\sigma_y$  vs  $1/\delta$ ), the heating effect is also negligible. Radiation heating, primarily ionization at short distance[5], from electrons passing

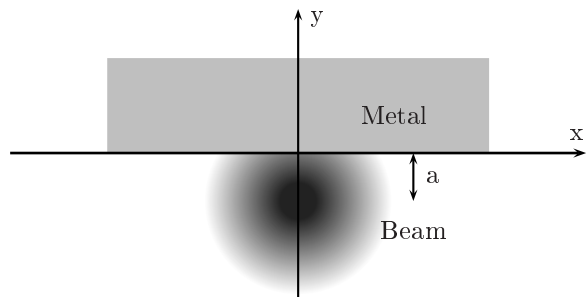


FIG. 6: Electron beam running into a metal surface.

through metal is an important source, which is considered at the end of the paper. From Eq. (3), the surface magnetic field reads

$$\tilde{H}_x(x=0, y=0, z, \omega) = \int_{-\infty}^0 dy \int_{-\infty}^{+\infty} \frac{\tilde{I}}{\pi} \frac{y dx}{y^2 + x^2}. \quad (18)$$

Integrating in  $x$ , we have

$$\tilde{H}_x(x=0, y=a, z, \omega) = -\frac{\tilde{I}(z, \omega)}{\pi\sqrt{\sigma_x\sigma_y}} f\left(\frac{a}{\sigma_x}, \frac{\sigma_y}{\sigma_x}\right), \quad (19)$$

where

$$\begin{aligned} f(u, v) &= \frac{1}{2\sqrt{v}} \int_0^\infty e^{-\frac{(u-w)^2}{2v^2}} e^{-\frac{w^2}{2}} \operatorname{erfc}\left(\frac{w}{\sqrt{2}}\right) dw, \\ \operatorname{erfc}(w) &= \frac{2}{\sqrt{\pi}} \int_w^\infty e^{-t^2} dt. \end{aligned} \quad (20)$$

In particular,

$$f(u, 1) = \frac{1}{2u} (\operatorname{erfc}(-\frac{u}{\sqrt{2}}) - e^{-u^2/2}). \quad (21)$$

The value of  $f(u, v)$  has one maximum as a function of  $u$  for every  $v$ . The maxima may be found numerically and its value  $f_{max}$  is fitted to the following function

$$f_{max}(v) \approx \alpha \sqrt{\frac{1}{2\pi}} \frac{\log(1 + \pi v)}{\sqrt{v}}. \quad (22)$$

The parameter  $\alpha$  is nominally 1, which gives the exact asymptotic limit for small and large  $v$ . Over the entire range of  $0 < v < \infty$ , this approximation gives the upper limit of  $f_{max}$ , and never more than 5.6% off. To be more accurate, a value of  $\alpha = 0.95$  produces no more than 0.5% relative error over the range of  $[0.25, 250]$ . A numerical solution of  $\alpha$  is plotted in Fig. 7 for reference, and in particular,  $f_{max}(1) = 0.54$  for a round beam.

Following Eq. 19, the maximum magnitude of the surface magnetic field becomes

$$\tilde{H}_x^{max} = \frac{\tilde{I}(z, \omega)}{\pi} \frac{f_{max}\left(\frac{\sigma_y}{\sigma_x}\right)}{\sqrt{\sigma_x\sigma_y}}. \quad (23)$$

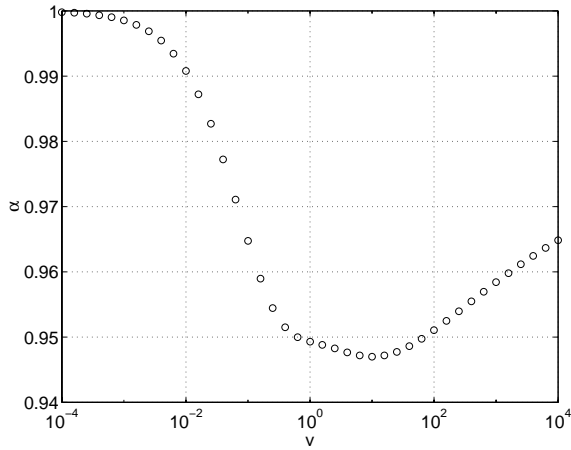


FIG. 7: Plot of the exact value of  $\alpha$  as a function of  $\nu$ .

The corresponding maximum surface temperature rise due to single bunch heating is

$$T_1^{max} = \frac{Z_0 c}{2\pi} \left(\frac{Q}{\sigma_z}\right)^2 \frac{f_{max}^2 \left(\frac{\sigma_y}{\sigma_x}\right)}{\pi^2 \sigma_x \sigma_y} \frac{1}{C_p}. \quad (24)$$

At the titanium spoiler, the transverse beam size  $\sigma_y = 60 \mu m$  and  $\sigma_x = 160 \mu m$ , giving a pulsed temperature rise of  $T_1^{max} = 2.83^\circ C$ .

#### IV. MULTI-BUNCH HEATING

Most of the new generation of accelerators are running in multi-bunch mode for efficiency and luminosity reasons. A nominal configuration calls for 90  $125 \mu m$  bunches spaced by about  $1.4 ns$ , and this bunch train, i.e. pulse, is repeated 120 times a second, as illustrated in Fig. 8.

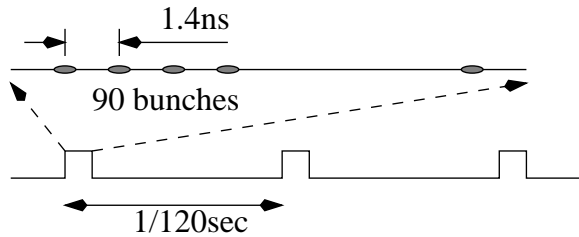


FIG. 8: bunch structure in modern collider.

In the previous section, we have shown that for single bunch, thermal diffusion length  $l_{diff}$  is always smaller than RF penetration depth  $\delta_e$ , therefore thermal diffusion is negligible. In the multiple bunch scheme, there are three regions of operation:

#### A short thermal diffusion length

If the thermal diffusion length of the bunch train is smaller than the RF penetration depth  $\delta_e$ , i.e.

$$l_{diff}^{train} = \sqrt{\frac{K N_p t_p}{C_p}} \ll \delta_e = \Gamma(3/4) \sqrt{2\sigma_z/c\mu\sigma}, \quad (25)$$

then

$$T_N(y) = N_p T_1(y), \quad (26)$$

where  $N_p$  is the number of bunches in a train, and  $t_p$  is the bunch separation. Here we have only considered the bunches within one pulse. The 120 Hz pulse structure is of secondary concern because the heat has mostly dissipated before the next bunch train arrives.

#### B long thermal diffusion length

However, in the above configuration,  $l_{diff}^{train}$  are  $3.8 \mu m$  and  $1.1 \mu m$  for copper and titanium respectively. While the effective skin depth  $\delta_e$  are  $0.117 \mu m$  and  $0.558 \mu m$  respectively. To the first order, we may assume  $l_{diff}^{train} \gg \delta_e$  and treat all the energy as deposited on the surface  $y = 0$ . This will over estimate the surface temperature slightly.

From Eq. (11), we can obtain the energy flux  $E_f$  deposited on the metal surface by a single bunch

$$\begin{aligned} E_f(x, y=0, z) &= \int_{-\infty}^{+\infty} \frac{d\omega}{2\pi} \int_0^{\infty} \tilde{P}_d dy \\ &= \left(\frac{Q}{\pi}\right)^2 \left(\frac{a}{a^2+x^2}\right)^2 \int_{-\infty}^{+\infty} \sqrt{\frac{\omega\mu}{2\sigma}} e^{-\omega^2/\omega_\sigma^2} \frac{d\omega}{2\pi} \\ &= \left(\frac{Q}{\pi}\right)^2 \left(\frac{a}{a^2+x^2}\right)^2 \sqrt{\frac{\mu}{2\sigma}} \left(\frac{c}{\sigma_z}\right)^{3/2} \frac{\Gamma(3/4)}{2\pi}. \end{aligned} \quad (27)$$

The one dimensional heat diffusion solution of a point source  $E_f \delta(y) \delta(t)$  is [6]

$$T(y, t) = \frac{E_f}{\sqrt{\pi K C_p t}} e^{-y^2/4Dt}, \quad (28)$$

where diffusion constant  $D = K/C_p$ . We can write the multi-bunch result as

$$T_N(y, t) = \sum_{n=1}^{N_p} E_f \frac{e^{-y^2/4D(t-nt_p)}}{\sqrt{\pi K C_p (t-nt_p)}} H(t-nt_p) \quad (29)$$

where  $H(t)$  is a step function with  $H = 1$  for  $t > 0$ , and zero otherwise. When  $N_p$  is large, the sum is approximated by an integral

$$T_N(y, t) = \int_0^t \frac{E_f e^{-y^2/4D(t-t')}}{\sqrt{\pi K C_p (t-t')}} H(N_p t_p - t') \frac{dt'}{t_p}, \quad (30)$$

which yields the surface temperature rise

$$T_N(0, N_p t_p) = \frac{2\sqrt{N_p} E_f}{\sqrt{\pi K C_p t_p}}. \quad (31)$$

Using Eq. (27) and substituting  $a/(a^2 + x^2)$  by  $f_{max}(\sigma_y/\sigma_x)/\sqrt{\sigma_x \sigma_y}$ , we have the maximum temperature rise induced by multi-bunch train

$$T_N^{max} = \frac{2\sqrt{N_p} Q^2}{\sqrt{\pi K C_p t_p}} \frac{f_{max}^2(\frac{\sigma_y}{\sigma_x})}{\pi^2 \sigma_x \sigma_y} \sqrt{\frac{\mu}{2\sigma}} \left(\frac{c}{\sigma_z}\right)^{\frac{3}{2}} \frac{\Gamma(\frac{3}{4})}{2\pi}. \quad (32)$$

The result has a characteristic  $\sqrt{N_p}$  growth of a diffusion solution. Taking the titanium collimator design as an example, the maximum multi-bunch heating will be  $T_N^{max} = 83.0^\circ C$ .

### C thermal diffusion length comparable with RF penetration depth

In the previous section, we assume that diffusion length  $l_{diff}^{train}$  is much larger than the RF penetration depth  $\delta_e$ , therefore the energy is treated as if deposited on the metal surface  $y = 0$ . A more accurate calculation takes the RF penetration into account. The temperature rise at  $y = 0$  due to a delta pulse energy density  $\delta(y - y')\delta(t - t')$  is [6]

$$T(0, t, y', t') = \frac{1}{\sqrt{\pi K C_p (t - t')}} e^{-y'^2/4D(t-t')}. \quad (33)$$

Then the surface temperature rise due to a single bunch

$$T_1(0, t, t') = \int_0^\infty E_d(y') \frac{e^{-y'^2/4D(t-t')}}{\sqrt{\pi K C_p (t - t')}} dy'. \quad (34)$$

From Eq. (12) we have  $E_d(y) = E_d(0)g(y/\delta_\sigma)$ . Using the exponential approximation for  $g$ , we can integrate Eq. (34) to obtain

$$T_1(0, t, t') = \frac{E_d(0)}{C_p} e^{\hat{x}^2} \text{erfc}(\hat{x}), \quad (35)$$

$$\hat{x} = \sqrt{4D(t - t')}/\delta_e.$$

At  $t = t'$ , it reduces to Eq. (16). Using the expansions

$$e^{x^2} \text{erfc}(x) = \frac{1}{\sqrt{\pi x}} \left[ 1 + \sum_{m=1}^{\infty} \frac{(2m-1)!!}{(-2x^2)^m} \right], \quad (36)$$

Eq. (35) becomes

$$T_1(0, t, t') = \frac{E_d(0)\delta_e/2}{\sqrt{\pi D(t - t')} C_p} \left[ 1 + \sum_{m=1}^{\infty} \frac{(2m-1)!!}{(-2\hat{x}^2)^m} \right]. \quad (37)$$

Noting that  $E_d(0)\delta_e/2$  equals the total energy flux deposited by the bunch, the first term of Eq. (37) reproduces the point source result. In this particular case, the

diffusion length in Ti between pulses,  $\sqrt{Dt_p} = 0.114\mu m$ , is smaller than the effective skin depth  $\delta_e = 0.558\mu m$ , the expansion does not converge very well for small  $\hat{x}$ . So we take Eq. (35) and sum over all the bunches,

$$T_N(0, t) = \frac{E_d(0)}{C_p} \sum_{n=0}^{N_p-1} e^{x_n^2} \text{erfc}(\hat{x}_n) H(t - nt_p), \quad (38)$$

$$\hat{x}_n = \sqrt{4D(t - nt_p)}/\delta_e.$$

The result, plotted in Fig. 9, gives  $T_N^{max} = 66.5^\circ C$ . It is about 20% lower than the simple estimation from Eq. (32).

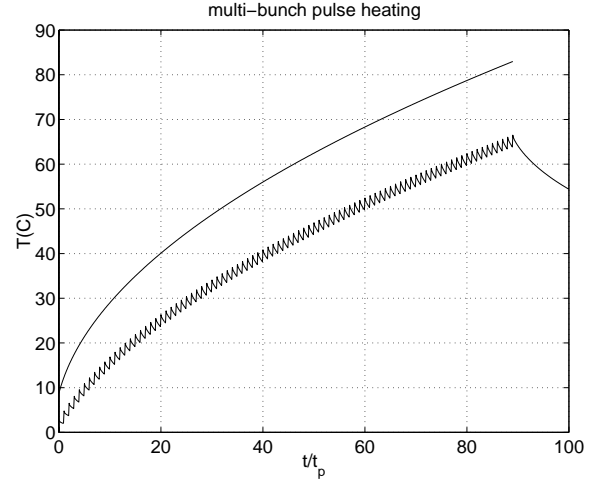


FIG. 9: Multi-bunch electron bunch heating for  $N_p = 90$ . The smooth approximation is from Eq. (32)

## V. SUMMARY

We have derived the image current heating on the metal surface due to charged pulses. The results are summarized in the following table.

TABLE I: Electron pulse heating from image current

	single bunch	multi-bunch heating
Temp rise	$T_1 = \frac{E_d(0)}{C_p}$	$T_N = \frac{E_d(0)}{C_p} \sum_{n=0}^{N_p-1} e^{x_n^2} \text{erfc}(x_n)$ $x_n = \sqrt{N_p - 1 - n} \frac{\sqrt{4Dt_p}}{\delta_e}$
$l_{diff}^{train} \ll \delta_e$		$T_N = \frac{N_p E_d(0)}{C_p}$
$l_{diff}^{train} \gg \delta_e$		$T_N = 2\sqrt{N_p} \frac{E_d(0)\delta_e/2}{\sqrt{\pi K C_p t_p}}$
Beam centered		$E_d(0) = \frac{Z_0 c}{2\pi} \left(\frac{Q}{\sigma_z}\right)^2 \left(\frac{1}{2\pi r_0}\right)^2$
Beam near surface		$E_d(0) = \frac{Z_0 c}{2\pi} \left(\frac{Q}{\sigma_z}\right)^2 \left(\frac{1}{\pi a}\right)^2$
Beam into surface		$E_d(0) = \frac{Z_0 c}{2\pi} \left(\frac{Q}{\sigma_z}\right)^2 \frac{f_{max}^2(\sigma_y/\sigma_x)}{\pi^2 \sigma_x \sigma_y}$

The pulsed heating due to charged bunches can be substantial with high peak current, small beam/structure

size and multiple bunches. A future linear collider spoiler design is shown to give  $66.5^\circ\text{C}$  temperature rise when a bunch train strikes it. This result should be compared to the corresponding radiation heating from electromagnetic showering and ionization. Assuming the spoiler is shorter than a radiation length and no thermal diffusion, i.e.  $\sigma_{x,y} \gg l_{diff}^{train}$ , the peak temperature is

$$T_{rad} = \frac{N_p(Q/e)dE/dx}{2\pi\sigma_x\sigma_y C_p}. \quad (39)$$

The energy deposition per unit length  $dE/dx \approx 7.2$  MeV/cm[7] for titanium, and the resulting  $T_{rad} = 728^\circ\text{C}$ . Under these parameters, radiation heating is much higher than that from image current. But it is notable that electron pulse heating  $T_N^{max}$  is proportional to  $(Q/\sigma_z)^2$  because of  $I^2R$  heating, while radiation heating is linear in  $Q$ . In situation of high peak current, image current heating will dominate. Taking the Linear Coherent Light Source as an example, the beam parameters are  $Q = 0.95$  nC,  $\sigma_x = \sigma_y = 38 \mu\text{m}$  and  $\sigma_z = 20 \mu\text{m}$ [8]. The Ti spoiler will suffer a pulsed temperature rise of  $T_1^{max} = 352^\circ\text{C}$  and  $T_{rad} = 31.9^\circ\text{C}$  when a bunch strikes it. Besides comparing temperature rise, one needs to keep in mind that electron pulse heating from image current is a surface phenomenon, while radiation heating is mostly a body effect. Therefore the mechanical effects and engineering requirements are different.

The above numerical examples show that the electron pulse heating due to image current is an important factor that need to be considered in future accelerator design.

The calculation in this paper has used 1-D thermal diffusion equation. For very long pulse and very small beam size, i.e.  $l_{diff}^{train} > \sigma_x$ , thermal diffusion and energy distribution in x direction (Fig. 6) may need to be considered. The result in Table. I can serve as an upper limit to the maximum temperature rise.

## VI. ACKNOWLEDGEMENTS

We would like to acknowledge Josef C. Frisch for suggesting this problem.

## APPENDIX A: OTHER OBSERVATIONS

The derived expression is also applicable to the case when a beam runs into metal surface at a steep angle, including but not limited to optical transition radiation (OTR) foils, wire scanners and beryllium windows. The surface magnetic field (Fig. 10) from a point charge is still given by Eq. 3. And the maximum surface magnetic field of a beam, Eq. 23, also applies, so do all the other equations. It is notable that the heating is independent of the angle  $\theta$ .

Taking a tungsten ( $C_p = 2.55\text{J/cm}^3$  and  $dE/dx = 22.7\text{MeV/cm}$ ) wire scanner at the LCLS as an example

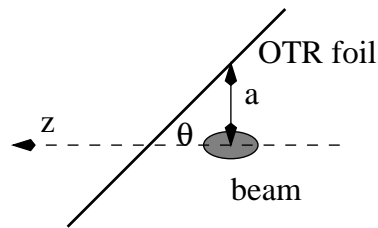


FIG. 10: beam passes through a OTR foil

(Fig. 11), the pulsed temperature rises due to image cur-

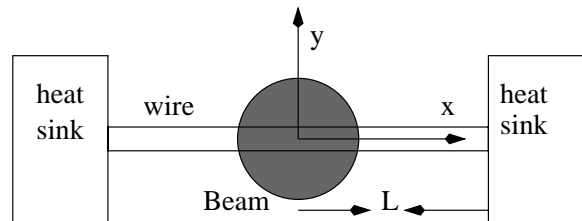


FIG. 11: beam passes through a wire scanner

rents and radiation are  $T_1^{max} = 325^\circ\text{C}$  and  $T_{rad} = 93.2^\circ\text{C}$  respectively. And it is on top of a equilibrium temperature of

$$T_{rad}^{eq} = \frac{(Q/e)dE/dx}{K} \frac{L}{\sqrt{2\pi}\sigma_y} PRR, \quad (A1)$$

where the wire is assumed to be much smaller than the beam size, and the Pulse Repetition Rate (PRR) is 120 Hz. The distance to heat sink  $L$  is assumed to be 1 cm. The total energy deposition from image current heating is ignored because it is a surface effect. The resulting  $T_{rad}^{eq} = 157^\circ\text{C}$ .

## REFERENCES

- [1] F.-J. Decker *et al.*, in *International Linear Conference (LINAC 1996)*, 18th, Geneva, Switzerland, Aug 26–30, 1996, edited by C. Hill and M. Vretenar (CERN, 1996), pp. 137–139.
- [2] A. P. Prudnikov, Y. A. Brychkov, and O. I. Marichev, *Integrals and series* (Gordon and Breach, 1986).
- [3] D. L. Burke *et al.*, *Zeroth-order Design for the Next Linear Collider*, Tech. Rep., Stanford Linear Accelerator Center (1996).
- [4] D. R. Lide, *Handbook of Chemistry and Physics*, 77th ed. (CRC press, 1996).
- [5] R. M. Barnett *et al.*, Phys. Rev. D **54**(1), 136 (1996).
- [6] X. E. Lin, in *Advanced Accelerator Concepts*, 8th, Baltimore, Maryland, July 6–11, 1998 (AIP, 1999), pp. 676–685.
- [7] R. B. Neal *et al.*, *The Stanford two-mile Accelerator* (W. A. Benjamin, 1968).

- [8] M. Cornacchia *et al.*, *LCLS Design Study Report*, Tech. Rep., Stanford Linear Accelerator Center (1998).
- [9] Using copper  $\sigma = 5.8 \times 10^7 / \Omega.m$ , but the inequality is true for most metal.